

ARTICLE OPEN



Broad sialic acid usage amongst species D human adenovirus

Rosie M. Mundy¹, Alexander T. Baker¹, Emily A. Bates¹, Tabitha G. Cunliffe¹, Alicia Teijeira-Crespo¹, Elise Moses¹, Pierre J. Rizkallah^{2,4✉} and Alan L. Parker^{1,3,4✉}

Human adenoviruses (HAdV) are widespread pathogens causing usually mild infections. The Species D (HAdV-D) cause gastrointestinal tract infections and epidemic keratoconjunctivitis (EKC). Despite being significant pathogens, knowledge around HAdV-D mechanism of cell infection is lacking. Sialic acid (SA) usage has been proposed as a cell infection mechanism for EKC causing HAdV-D. Here we highlight an important role for SA engagement by many HAdV-D. We provide apo state crystal structures of 7 previously undetermined HAdV-D fiber-knob proteins, and structures of HAdV-D25, D29, D30 and D53 fiber-knob proteins in complex with SA. Biologically, we demonstrate that removal of cell surface SA reduced infectivity of HAdV-C5 vectors pseudotyped with HAdV-D fiber-knob proteins, whilst engagement of the classical HAdV receptor CAR was variable. Our data indicates variable usage of SA and CAR across HAdV-D. Better defining these interactions will enable improved development of antivirals and engineering of the viruses into refined therapeutic vectors.

npj Viruses (2023)1:1; <https://doi.org/10.1038/s44298-023-00001-5>

INTRODUCTION

Human adenoviruses (HAdV) are classified phylogenetically into seven species, A–G, based classically on testing for neutralizing activity by serological analysis^{1,2}. They are highly diverse, and have become of great interest for their use as therapeutic vectors and vaccines. Adenoviruses are non-enveloped viruses and have a double stranded DNA genome of around 35 kb, which lends itself readily to genetic manipulations³. These manipulations allow them to be tailored into safe and effective delivery platforms for gene therapy and oncolytic payloads which, coupled with their good safety profile, make them attractive targets for therapeutic development.

Adenoviruses have a highly conserved structure⁴. Their icosahedral capsid is made up of three major proteins: the hexon, penton and fiber, in addition to other minor and cement proteins. Each protein forms key interactions to promote cell infection, with the terminal domain of the fiber, the fiber knob protein, interacting with the viruses' primary cell entry receptor.

Therapeutic development has historically focused significantly on the archetype species C adenovirus type 5 (HAdV-C5). However, the use of this virus faces many hurdles including high pre-existing seroprevalence rates in some populations, as well as undesirable interactions with blood components such as blood clotting factors^{5,6}, which may reduce efficacy and promote off target toxicities of platforms based on HAdV-C5^{7–9}. Species D adenoviruses (HAdV-D) represent alluring alternatives, with generally lower rates of pre-existing immunity in Western populations, however they are severely understudied when compared to others, such as the species C adenoviruses.

Species D adenoviruses generally cause ocular and gastrointestinal infections, including HAdV-D8, which recently caused an outbreak of conjunctivitis in Leicester, UK¹⁰. They can also cause epidemic keratoconjunctivitis (EKC), which is endemic to Japan and causes a strain on the healthcare system¹¹. The lack of understanding on species D viruses' basic mechanisms of cellular

infection prevents better treatment of these diseases, and clarification would allow generation of more effective therapeutics.

Previous work has demonstrated that species D adenovirus 26 (HAdV-D26) fiber knob protein does not engage classical proteinaceous receptor CD46, and only weakly binds Coxsackie and Adenovirus Receptor (CAR), where its engagement is sterically hindered by an extended DG loop, blocking this interface. Instead, the HAdV-D26 fiber knob protein engaged sialic acid with high affinity as a cell entry receptor^{12,13}. HAdV-D26 has been used extensively clinically as vaccines against Ebola¹⁴, HIV¹⁵ and most recently SARS-CoV-2¹⁶. Interactions with sialic acid have been described with other species D adenoviruses including adenovirus 19p (HAdV-D19p), 37 (HAdV-D37) and 64 (HAdV-D64)^{17–19}. Sialic acid is also known to be commonly used in other virus infection mechanisms such as influenza and is the terminal residue of complex glycan chains on a large proportion of vertebrate cell surfaces, including humans²⁰. All of the aforementioned viruses bind sialic acid in an apical binding pocket, despite HAdV-D26 fiber knob protein having a different electrostatic profile and low sequence similarity to the others¹², suggesting the potential for widespread usage of the receptor across the species D adenoviruses. We assessed the ability for HAdV-D to engage sialic acid and CAR as cell entry receptors via an integrative structural biology workflow, suggesting a species wide dual tropism,

RESULTS

High resolution crystal structures confirm conserved structure of species D adenovirus fiber knob proteins

Adenovirus fiber knob proteins crystallised readily, under widely varying pH conditions. The achieved resolution is mostly very high, up to 1.37–1.6 Å, although some species gave diffraction to a more modest resolution. Details of data collection and refinement are presented in Supplementary Tables 1–4.

The adenovirus fiber knob protein is known to have a highly conserved trimeric structure. We performed X-ray crystallography to

¹Division of Cancer & Genetics, Cardiff University School of Medicine, Cardiff CF14 4XN, UK. ²Division of Infection & Immunity, Cardiff University School of Medicine, Cardiff CF14 4XN, UK. ³Systems Immunity University Research Institute, Cardiff University School of Medicine, Cardiff CF14 4XN, UK. ⁴These authors contributed equally: Pierre J. Rizkallah, Alan L. Parker. ✉email: RizkallahP@Cardiff.ac.uk; ParkerAL@Cardiff.ac.uk

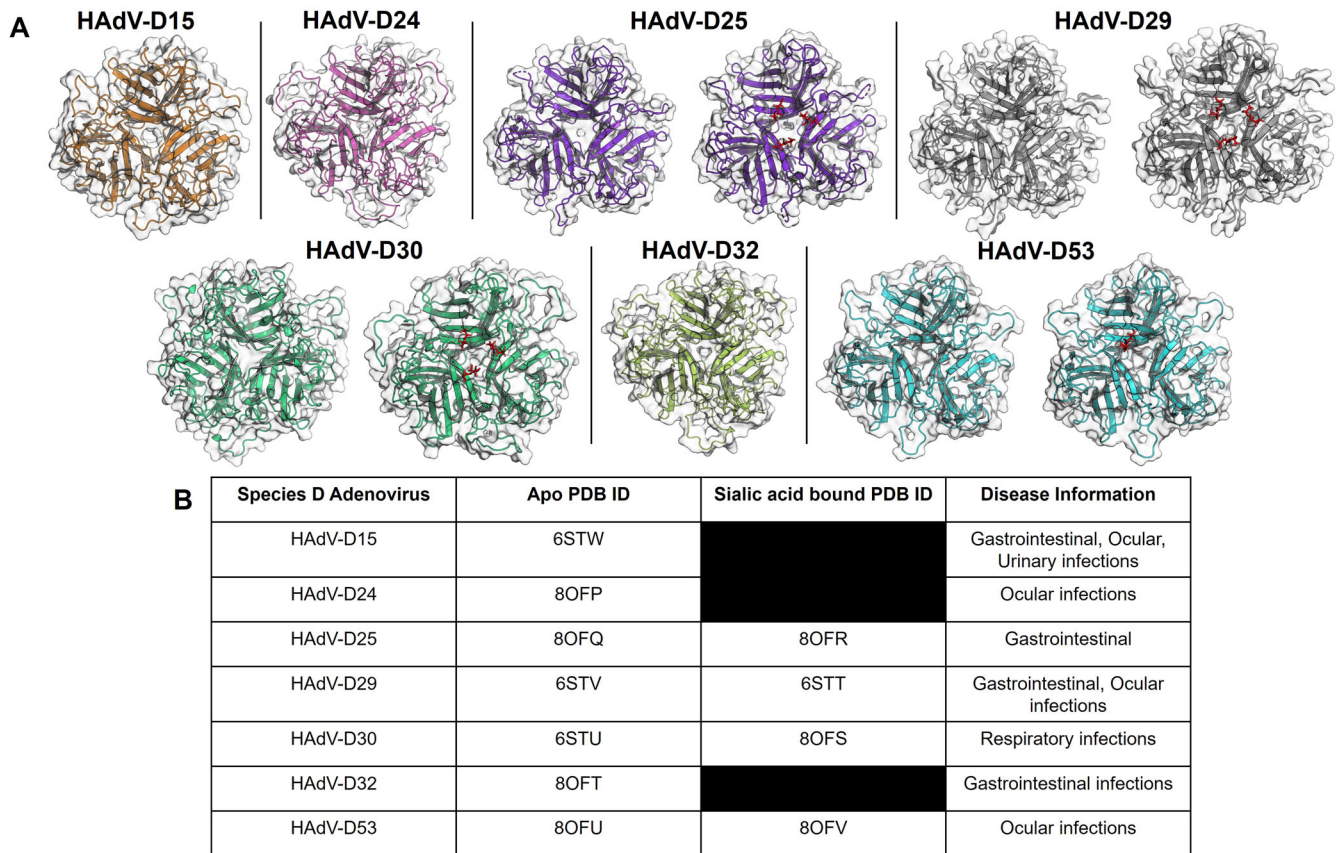


Fig. 1 Crystallisation of species D fiber-knob proteins (Charles et al. 1995; Shieh. 2022; Walsh et al. 2009; Van der Veen and Van der Ploeg. 1960; Faden et al. 2005). Adenovirus species D fiber-knob proteins are presented in their apo states in (A). HAdV-D15, D24 and D32 were crystallised in only their apo states, whereas HAdV-D25, D29, D30 and D53 crystals were also soaked with sialic acid. These structures are shown side by side, with sialic acid highlighted in red. (B) Presents the PDB IDs and relevant disease information for each of the species D fiber-knob proteins crystallised.

generate structures of species D human adenovirus fiber knob proteins HAdV-D15, D24, D29, D30, D32 and D53 in their apo states. These structures show the expected trimeric form, all viewed down towards the apical domain of the fiber knob proteins (Fig. 1).

To evaluate the potential for these recombinant fiber knob proteins to bind cellular sialic acid residues, crystals of the fiber-knob proteins were also soaked with sialic acid prior to data collection. This resulted in four structures of HAdV-D25, D29, D30 and D53 in complex with sialic acid also shown in Fig. 1. Sialic acid was observed to bind within a conserved apical region, as observed previously in structures solved for sialic acid interacting species D adenoviruses, including HAdV-D26 (PDB ID: 6QU8) and HAdV-D37 (PDB ID: 1UXA).

The observed space groups were monoclinic (P₂₁, P2 or C2), orthorhombic (P2₁2₁2₁), trigonal (H3 – R3 in hexagonal axes) or cubic (P23). However, there were varying numbers of monomers or trimers in each asymmetric unit, presenting a diverse picture of the fiber knob interactions. HAdV-D24 fiber knob crystals achieved only marginal resolution, and soaking rendered them too disordered for diffraction. Additionally, crystals of HAdV-D32 fiber knob protein soaked with sialic acid could not be obtained.

The conformation of the bound sialic acid was found to be a mixture of the α and β anomers, freely exchangeable in solution and minimal protein side chain adjustment was required to accommodate either conformation. Soaking in sialic acid containing solutions reduced resolution slightly. Crystals of HAdV-D53 fiber knob protein were too sensitive to soaking, and only very short soaks could rescue any samples suitable for diffraction. The short soak allowed only two of four trimers in the asymmetric unit

to bind β -sialic acid, with a significant change in packing, explaining the sensitivity of these crystals to soaking.

These adenoviruses are of significant clinical relevance (Fig. 1B). They cause gastrointestinal and ocular infections of varying severity. HAdV-D53 is of particular interest due to the recent confirmation of EKC causing infection, similar to previously identified sialic acid binding viruses HAdV-D37 and D64.

Conserved residues mark the sialic acid binding pocket

A consensus binding pocket, including bridging waters, was identified in the HAdV-D26 fiber knob protein in complex with sialic acid (PDB ID: 6QU8) anchoring sialic acid in place¹². The new structure determinations could not identify the same number of contacts throughout, due to the inability to locate water molecules at different resolutions. Figure 2A–E depicts these pockets in fiber knob proteins of HAdV-D25, D29, D30 and D53, where sialic acid is coloured according to structure and the residues contacting sialic acid are shown in green. Other pocket residues not making contact with sialic acid are shown in red. Figure 2F shows an alignment of the sialic acid binding fiber knob proteins, highlighting contacting residues in yellow compared to the binding pocket identified in HAdV-D26. Y314 and K349 (according to HAdV-D26 sequence) are conserved across all sequences, while the remaining residues are similar, suggesting the existence of a common sialic acid binding pocket across all species fiber knob proteins. Y237 and K349 have also been previously seen to interact in a structure of HAdV-D37 fiber knob protein interacting with sialylactose¹⁸.

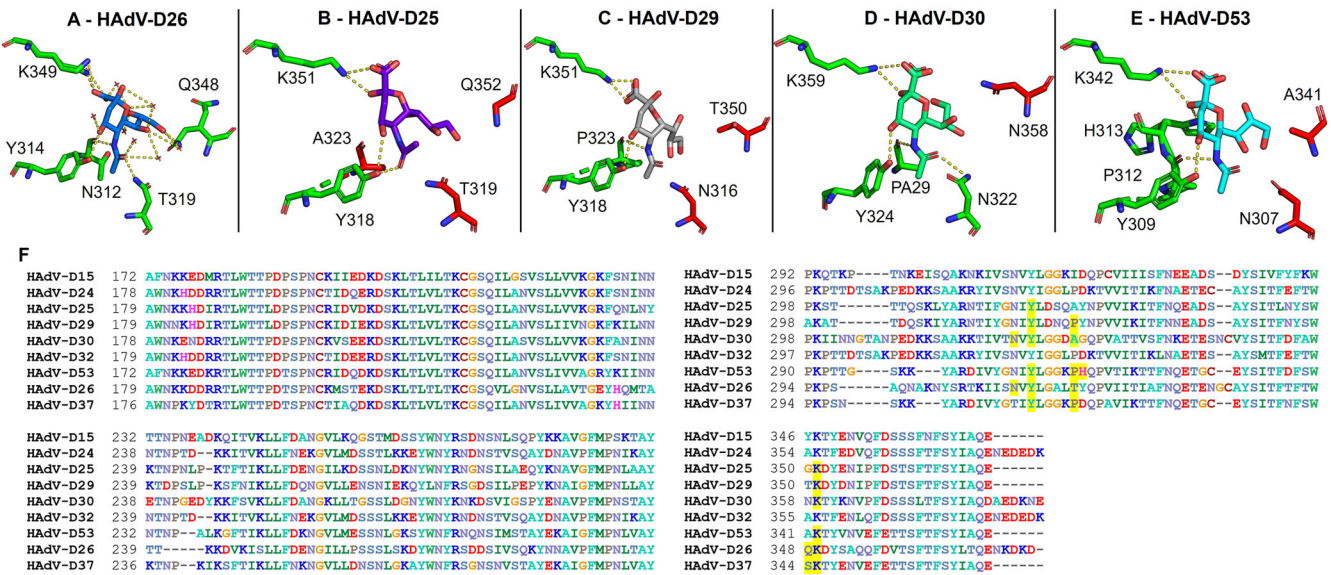


Fig. 2 Species D adenoviruses have conserved sialic acid binding residues. Panel (A) shows the sialic acid binding pocket of HAdV-D26 (PDB ID: 6QU8). For all structures, interacting residues are highlighted in green with interactions represented in yellow dashed lines. Residues that are not interacting with sialic acid are highlighted in blue. Nitrogen elements are shown in blue, with oxygen elements in red. Sialic acid soaked structures are shown for HAdV-D25 (B), D29 (C), D30 (D) and D53 (E). Panel (F) presents an alignment of the fiber-knob region of species D fiber-knob proteins coloured according to residue. Residues highlighted in yellow are shown to be interacting with sialic acid by crystal structure (PDB ID: 1UXA for HAdV-D37 interactions).

Removal of cell surface sialic acid with neuraminidase reduces the transduction of pseudotyped species D adenoviruses

Following structural investigation of species D adenovirus fiber-knob proteins, *in vitro* cell based assays were used to biologically validate the importance of the identified interactions with sialic acid. Pseudotyped viruses comprising an HAdV-C5 core viral vector pseudotyped with the fiber knob proteins of several HAdV-D of interest (D26, D15, D24, D29 and D53) were generated expressing a luciferase transgene under the control of a ubiquitous CMV IE promoter for measuring transduction following cell treatment with and without neuraminidase treatment.

We used a control, HAdV-C5 expressing luciferase, which has a well characterised and high affinity interaction with CAR that is not influenced by sialic acids²¹. Alterations in transduction mediated by HAdV-C5 were non-significant as observed across all three cell lines, with a small increase in transduction observed in CAR^{LOW} BT-20 cells (Fig. 3A). In contrast, viruses pseudotyped with the fiber-knob protein of HAdV-D26 demonstrated a statistically significant reduction in transduction in all cell lines following cleavage of sialic acid (Fig. 3B). This was also demonstrated by viruses pseudotyped with an HAdV-D53 fiber knob protein (Fig. 3F), where all reductions in transduction were also statistically significant in all three cell lines tested.

Non-significant changes in transduction were observed when cells were transduced with viruses with the fiber-knob proteins of HAdV-D15, D24 and D29 (Fig. 3C–E). There was an overall trend in reduction, although in BT-20 cells there was a small, non-significant, increase in transduction of HAdV-D29 fiber-knob protein virus following treatment with neuraminidase. These results indicate significant usage of sialic acid by HAdV-D53 fiber-knob proteins, and the potential partial usage across the other species D adenovirus fiber-knob proteins.

Characterisation of species D adenovirus fiber knob proteins interactions with CAR

Since CAR is also known to be partially engaged by knob proteins of adenoviruses from HAdV-D including HAdV-D10, D26 and

D48^{13,22}, we additionally performed binding assays to investigate interactions of species D adenoviruses with CAR (Fig. 4). The classical CAR binding adenovirus fiber-knob protein, HAdV-C5, binds CAR with high affinity, with a measured value of 0.0001804 $\mu\text{g}/10^5$ cells. CAR binding was investigated for fiber knob proteins of HAdV-D24, D26 and D32, and was found to be significantly weaker interacting. The respective IC₅₀ values were quantified as 0.02931, 0.001261 and 0.01996 $\mu\text{g}/10^5$ cells. These values represent fold changes of 162, 6 and 110 times weaker compared with the IC₅₀ value measured for HAdV-C5 fiber knob protein.

The fiber knob protein of HAdV-D53 was also investigated for its ability to interact with CAR. An accurate IC₅₀ value could not be measured due to a lack of ability to block CAR antibody binding, even at the highest doses tested. This data suggests variable usage of CAR across the species D adenoviruses' fiber-knob proteins with some capable of interacting more strongly with CAR than others.

Inability of HAdV-C5 to bind sialic acid despite apparently conserved residues in the binding pocket

To confirm the validity of our structural observations, we used as a negative control of our structural modelling. We used the fiber-knob protein of HAdV-C5 (PDB ID:6HCN) superposed on the binding pocket of HAdV-D26 (PDB ID: 6QU8) (Fig. 5). We observed conservation of binding residues, with the HAdV-C5 chain shown (red) and HAdV-D26 (green) and interactions between sialic acid and HAdV-C5 shown (yellow).

There is also replacement of T319 with K526 in HAdV-C5, which extends away from the sialic acid in the binding pocket. Whilst the threonine was not found to be universally conserved (Fig. 2F), the other species D adenoviruses had similar sized residues which generally made interactions with sialic acid in HAdV-D29, D30 and D53 (Fig. 2C–E). This contrasts with the lysine seen in the same position in HAdV-C5 which prevents HAdV-C5 binding to sialic acid through steric hindrance. Overall, the residues in the binding pocket in HAdV-C5 are shown to differ from those seen in the

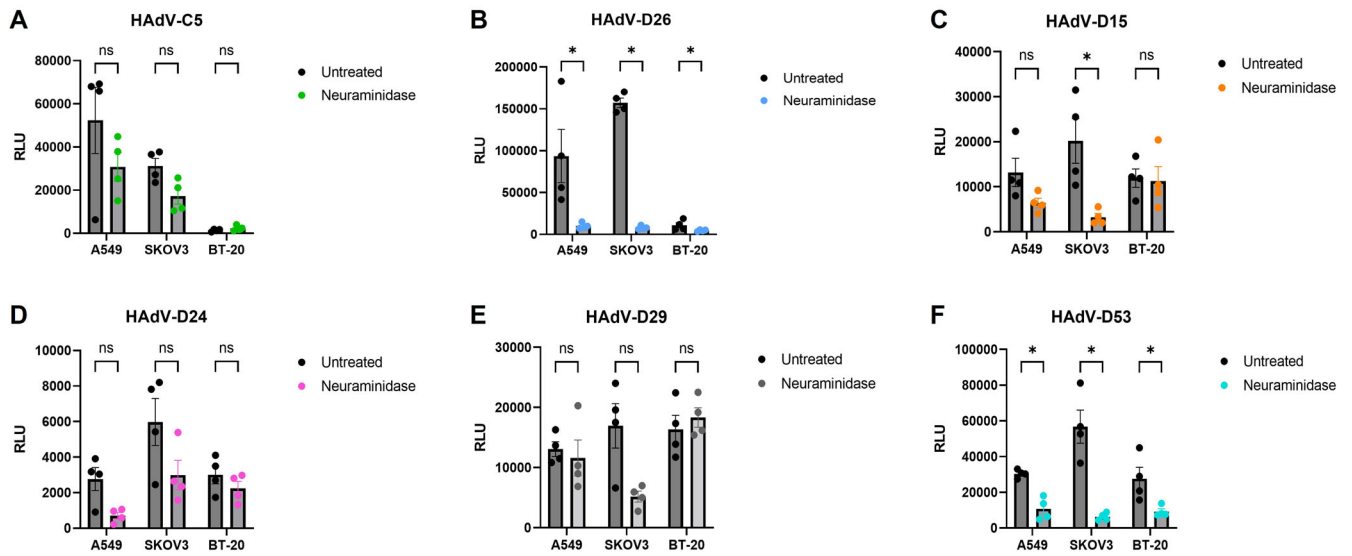


Fig. 3 Treatment by neuraminidase reduces transduction of pseudotype species D adenoviruses. A549, SKOV3 and BT-20 cell lines were each infected with luciferase-expressing adenovirus at 5000VP/cell. Panel (A) shows non-significant interaction with HAdV-C5 as a negative control, whereas panel (B) shows statistically significant reduction in transduction by pseudotype HAdV-C5 with a HAdV-D29 fiber-knob protein across all three cell lines. Panels (C–F) present the result of neuraminidase treatment by HAdV-C5 with HAdV-D15, D24, D29 and D53 fiber-knob proteins respectively. Error bars present standard error, and data was statistically tested by Mann-Whitney test ($n = 4$). ns (not significant) - $p > 0.05$, * - $p < 0.05$.

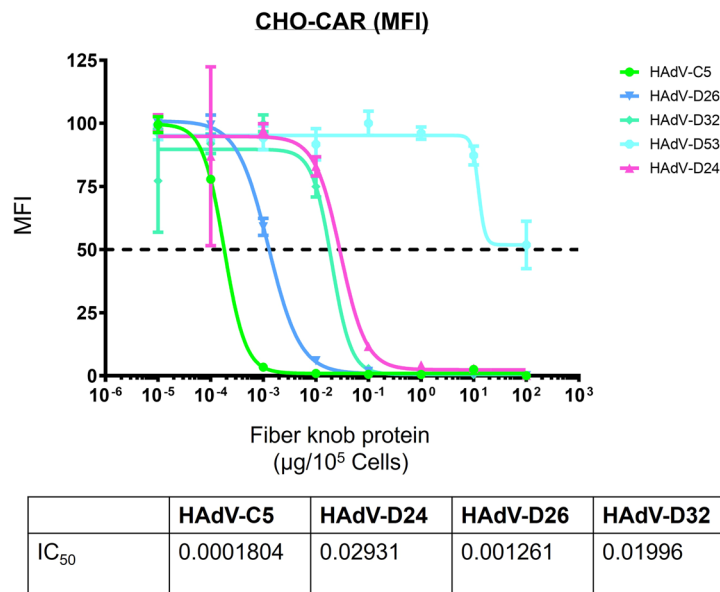


Fig. 4 IC_{50} curves suggest varied usage of CAR by species D adenoviruses. Using CHO-CAR cells, adenovirus fiber-knob proteins were tested for interaction with CAR and HAdV-C5 had the strongest IC_{50} value as the positive control. HAdV-D24, D26 and D32 fiber-knob proteins had weaker IC_{50} values but could still interact with CAR. HAdV-D53 fiber-knob protein could not give a reliable IC_{50} value.

binding pockets in Fig. 2, highlighting key differences between sialic acid utilising viruses, and those known to use different receptors such as CAR. This suggests that the sialic acid binding pocket identified in species D adenovirus fiber-knob proteins is not universal across all species and may be a unique feature of HAdV-D.

DISCUSSION

Sialic acid is well characterised as a primary cell receptor for a wide range of viruses including influenza and some coronaviruses, in addition to human adenoviruses²³. Previous studies have identified

sialic acid interactions with individual species D viruses including HAdV-D26, 37 and 64^{12,17,19}. Low sequence similarity in the fiber-knob protein has been seen to be tolerated to still allow usage of sialic acid cell entry¹², hinting at broader usage of sialic acid across HAdV-D. Although there is clear sequence variation across the proteins, we observed conservation of key sialic acid binding residues as highlighted in the alignment and the individual crystal structure for each complexed protein (Fig. 2A–E). The fiber-knob protein initiates cell entry by human adenoviruses and so binding here is critical for infection. These interactions are pivotal in defining a viral tropism, and knowledge of these interactions can aid in design of antivirals for therapeutic purposes. It should be

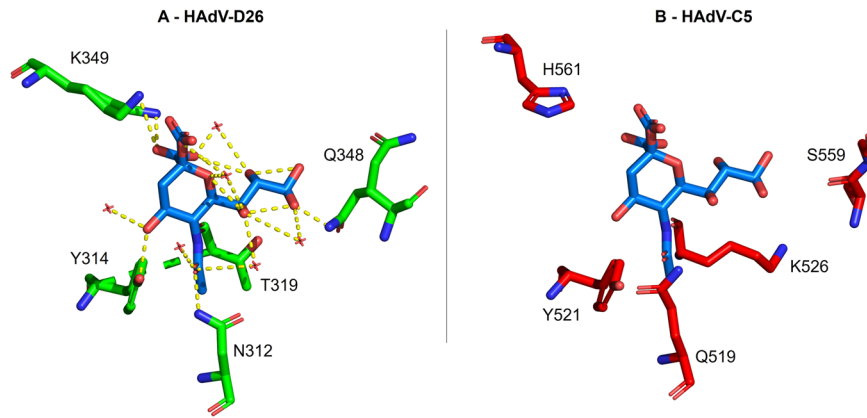


Fig. 5 HAdV-C5 fiber-knob protein is incompatible with sialic acid interaction. In panel (A), The sialic acid binding pocket of HAdV-D26 (PDB ID: 6QU8, shown in green) was aligned to the fiber-knob protein of HAdV-C5 (PDB ID: 6HCN, shown in red) in panel (B) and important residues highlighted. Nitrogen elements are shown in blue with oxygen in red. Many of the residues important in HAdV-D26's interaction with sialic acid are not present in HAdV-C5, such as the anchoring lysine, preventing interaction with sialic acid.

noted that another adenovirus from a different species has also been identified as binding sialic acid. Species G virus HAdV-G52 fiber-knob protein binds sialic acid, however, it does so at a different binding site on the side of the fiber-knob protein²⁴. This further suggests the apical binding pocket may be specific to the species D adenoviruses, whilst alternative means to engage sialic acids may be conserved across other species.

Figure 5 highlights the differences between HAdV-D26 and HAdV-C5 in the sialic acid binding pocket. Y314 in HAdV-D26, identified in Fig. 2 as being universally conserved in species D adenovirus fiber-knob proteins is conserved while K349 is replaced by a histidine in HAdV-C5, a much shorter side chain. This fails to contact sialic acid, weakening the sialic acid pocket which, alongside other substitutions of amino acids shown in Fig. 5, makes HAdV-C5 unable to engage sialic acid as species D adenoviruses can. We speculate that K349 is important and so the substitution to H561 in HAdV-C5 hinders the latter virus' ability to engage sialic acid as a cell entry receptor.

Previous studies have identified an ocular tropism in humans common among sialic acid utilising viruses²⁵. The species D adenoviruses generally cause rare gastrointestinal or ocular infections (Fig. 1B). Many previously identified species D viruses that utilise sialic acid cause EKC, the most severe form of human adenovirus caused conjunctivitis²⁶. Particularly contagious, EKC is characterised by its involvement of the cornea, can result in blindness and is notoriously difficult to treat with the potential to cause chronic disease²⁷. One of the viruses in this article that demonstrated significantly reduced transduction on removal of sialic acid following neuraminidase treatment is HAdV-D53 (Fig. 3F). This virus has been confirmed to also cause EKC and has been isolated from patients in Germany and Japan^{28,29}. The species D adenoviruses are notable for their frequent recombination events and when investigated, HAdV-D53 seemed to have arisen from HAdV-D22 recombining with two sialic acid binding, EKC causing adenoviruses: HAdV-D8 and D37^{28,29}. This recombination event, combining two viruses with similar tropisms explains our findings that HAdV-D53 appears to rely heavily on sialic acid as a cell entry receptor (Figs. 2E, 3F). HAdV-D37 has also been involved in recombination events leading to other EKC causing adenoviruses such as HAdV-D64, previously HAdV-D19a³⁰, drawing another similarity between the EKC causing adenoviruses.

The variation in sialic acid and CAR usage seen across the species D viruses investigated in this article suggests that the viruses within this species may not rely on a single receptor for initiating cell infection. The species C viruses have well-defined primary cell entry receptor interactions with CAR²¹. The interactions between HAdV-C5 and CAR is especially well

characterised, as HAdV-C5 forms the basis of many vectors in previous and current clinical trials including as a vaccine platform for COVID-19 and as a vector in a newly approved therapy for bladder cancer^{31,32}. In contrast, HAdV-B viruses display dual receptor usage similar to our observations of the species D adenoviruses in this article and are known to use both CD46 and in some cases, desmoglein-2 (DSG-2)^{33,34}. It is clear from the data in Fig. 3 that a single species wide receptor is unlikely for HAdV-D. This led us to investigate whether dual receptor usage was employed by HAdV-D.

The classical human adenovirus receptor, CAR, is over-expressed on CHO-CAR cells used for our binding experiments (Fig. 4) which demonstrated variable affinity of species D fiber-knob proteins for CAR. As expected, this interaction was much weaker than that of HAdV-C5 fiber-knob protein. Fiber-knob proteins of HAdV-D24, D26 and D32 all had a much weaker IC₅₀ value, with HAdV-D53's fiber-knob protein seemingly unable to interact with CAR. This again suggested a range of variability, with some viruses such as HAdV-D53 having a clear preference for sialic acid primarily but others demonstrating the ability to interact with both receptors.

Sialic acids are a family of terminal monosaccharides at the end of the glycan chains that decorate many vertebrate cells, making it a highly biologically relevant receptor but also a receptor of variable nature making it difficult to investigate²⁰. This means we must also consider the possibility that variation in glycan chains could change the ability for usage by species D adenoviruses. Few viruses are known to have a glycan chain preference, with HAdV-D37 known to preferentially bind GD1a glycan³⁵ and so it is important to consider this when interpreting our results as different fiber-knob proteins may have a preference for glycosylation patterns which may affect their usage of sialic acid and CAR. This is all before considering secondary interactions with the hexon and penton proteins of the adenovirus capsid demonstrating the complexity of this interaction and the difficulty in defining it. It should also be noted that we used both α and β conformers of sialic acid to soak the crystal structures presented in Fig. 2, although the β -conformer would not ordinarily be present in eukaryotic oligosaccharides.

Soaking our fiber-knob protein crystals allowed direct investigation into the potential for sialic acid to interact in the previously identified binding pocket. In contrast, modelling this interaction *in silico* could have reduced the accuracy that comes with X-ray crystallography. In this article we present seven novel structures of apo state fiber-knob proteins of species D adenoviruses (Fig. 1A). These provide a good basis from which to conduct structural analyses. However, the four sialic acid soaked novel crystal structures (Fig. 2B–E), provide a much more reliable view of the

binding pocket and interactions with sialic acid. However, it is important to remember that crystallography shows only a snapshot of the interaction, and not a dynamic model. This limitation encouraged the usage of an integrated structural biological workflow, to couple our structural observations with biologically measured effects.

By studying a virus' protein structure we can begin to elucidate it's basic mechanisms of cellular infection. This can confer benefits in two main applications. Primarily, understanding such mechanisms is vitally important when designing antivirals to combat the virus and the diseases they cause. In the case of EKC causing viruses, infection can result in chronic disease costing healthcare providers huge amounts over patients' lifetimes and drastically reducing patients' quality of life²⁶. The second application considers the therapeutic potential of species D adenoviruses. Traditionally HAdV-C5 has been the basis of many adenovirus derived vectors, however, the virus has high seroprevalence in many populations resulting in high levels of neutralising antibodies³⁶. The rarity of infections by species D adenoviruses means there is low pre-existing immunity to the viruses and so they could be effective alternative platforms to HAdV-C5. There is already some precedence to using species D adenoviruses in therapeutics, with HAdV-D26 being used as a vaccine platform to combat Ebola, HIV and SARS-CoV2 infections^{37–39}. We can only achieve these two benefits if we have a solid basis of understanding of these viruses which is where studies investigating structure and function can help to build a profile of each individual virus, to ameliorate its burden on both patient and healthcare system but also to utilise the virus to our advantage in a therapeutic setting.

Future work in this area should focus on defining the preference of the individual species D adenoviruses for each receptor. This article highlights the variation across this species, unlike the highly conserved tropisms seen across species B and C viruses^{11,33}, and therefore it is likely that each individual virus will need to be profiled prior to the design of antivirals or usage as a therapeutic vector. Previous studies have highlighted the species D viruses' rarity of infection⁴⁰ and therefore their lack of neutralising antibodies present in patients. Thus, they represent a promising option for future therapeutics, but must be properly vetted prior to being used as vectors.

Our findings demonstrate a conserved binding site for sialic acid, common across the species D adenoviruses, therefore suggesting that, along with CAR, the receptor can be used to initiate cell entry. When comparing to previously known sialic acid binders, we can appreciate how the diversity of sequence across the species D fiber-knob proteins is tolerated and still permits interaction with sialic acid. We validated our structural data with *in vitro* assays which confirmed species D fiber-knob proteins were capable of interacting with both CAR and sialic acid, raising the possibility of variable usage of both receptors across the species. This will be important when designing antiviral drugs for the species D viruses, especially those such as HAdV-D37 and D53 which have the capability to cause EKC creating a large burden on healthcare systems. On a wider basis, the species D viruses have great potential as therapeutic vectors but more must be done to understand their mechanisms of infection prior to them being used in the clinic.

METHODS

Generation and purification of recombinant fiber knob proteins

pQE expression plasmids (Qiagen, Manchester, UK) containing DNA encoding species D fiber knob proteins were produced by TWIST Biosciences (San Francisco, USA). The vectors were transformed by heat shock into competent SG13009 *Escherichia*

coli (*E.coli*) bacteria containing a pREP4–4 plasmid. Heat shock transformation was performed by heating the SG13009 *E.coli* and pQE-30 vectors at 42 °C in a waterbath for 30 s and cooling on ice for 2 min.

250 µL of room temperature SOC media (Super Optimal Broth with added glucose) was added and bacteria recovered in a shaking incubator for 1 h at 37 °C. Transformed bacteria were spread on LB-agar plates with 100 µg/mL Kanamycin and 50 µg/mL Ampicillin and grown overnight at 37 °C. Transformed colonies were confirmed by sequencing. SG13009 colonies containing the appropriate species D pQE fiber knob protein expression vectors were cultured to an optical density of 0.6 in Terrific Broth (TB, Sigma-Aldrich, Gillingham, UK), harvested by centrifugation and purified by nickel immobilised metal affinity chromatography (IMAC) and size exclusion chromatography (SEC) as described previously in ref. ¹².

Fiber knob protein crystallisation

All crystal plates used the Pact Premier Screen (Molecular Dimensions, Suffolk, UK). EasyXtal 15-well Tool crystal plates (Qiagen, Manchester, UK) were set up manually for HAdV-D15, D29 and D30 using the hanging drop method. Drops at either ratios of 1:1 or 3:1 (protein to screen) were suspended over a 300 µL reservoir. Crystal plates for HAdV-D24, D25, D32 and D53 fiber-knob proteins were set up using a Mosquito crystallisation robot (SPT Labtech, Hertfordshire, UK) for preliminary work, while optimisation and sialic acid soaking experiments were also performed using manually set up plates.

Plates were sealed and incubated at 18 °C for between 7 and 21 days. Crystals of HAdV-D25, D29, D30 and D53 were soaked before harvest with N-Acetyl Neuraminic Acid (Sigma-Aldrich, Gillingham, UK) at a concentration of 10 mM.

Crystals were harvested on litholoops (Molecular Dimensions, Suffolk, UK), flash frozen in liquid nitrogen, and transported to the Diamond Light Source where diffraction data were collected on Beamline I03 for HAdV-D15, D25, D29 and D30 and Beamline I04 for HAdV-D24, D25 (with and without sialic acid), D29 soaked with sialic acid and D30 soaked with sialic acid. Data for HAdV-D32 and D53 (with and without sialic acid) were collected on Beamlines I03, I04 and I04–1. During data collection, crystals were maintained at 100 °K.

Structure determination

Diffraction patterns were recorded and reduced automatically through the Diamond Light Source pipeline with XDS⁴¹, xia2 DIALS and 3dii⁴². Scaling and merging data was completed with Pointless, Aimless and Truncate while MolREP and Phaser were used for structure solving. All of these programs are included in the CCP4 Program package⁴³. RefMac5 was used for map generation and refinement and WinCoot was used for sequence adjustments and model corrections. PyMOL Version 2.2.3 was used to generate illustrations of crystal structures and models⁴⁴.

Fiber-knob protein sequence alignment

Sequences for species D fiber-knob proteins were obtained from NCBI and aligned using Clustal Omega⁴⁵. The output was displayed in BioEdit.

Cell culture

Cells were obtained from the American Type Culture Collection (ATCC) or collaborators. Cells were passaged twice weekly to maintain a confluency at less than 70% until used in an assay. All cells were cultured at 37 °C with 5% CO₂. SKOV3 cells (obtained from ATCC) were cultured in DMEM (Sigma-Aldrich, Gillingham, UK), A549 cells (also obtained from ATCC) were cultured in RPMI 1640 (Sigma-Aldrich, Gillingham, UK) and BT-20 cells (Obtained

from Dr Lynda Coughlan, University of Glasgow) were cultured in α -MEM (Gibco, ThermoFisher Scientific, Waltham, USA). All media was supplemented with 10% fetal bovine serum and 2% penicillin and streptomycin. RPMI 1640 was also supplemented with 1% L-glutamine.

Neuraminidase assay

Human cancer cell lines SKOV3, A549 and BT-20 were seeded at 5×10^4 cells per well in Nunclon Deplat Surface 96 well flat-bottomed cell culture plates (Thermo-Fisher Scientific, Waltham, USA). Cells were left to adhere overnight under normal cell culture conditions. Cells were washed with 200 μ L PBS before neuraminidase (Sigma-Aldrich, Gillingham, UK) was added at 50 mU/mL for 1 h at 37°C. Wells were washed with 200 μ L PBS before 100 μ L of replication deficient, luciferase expressing pseudotyped virus in serum free media was added at a viral particle titer of 5000 VP/cell in triplicate. Plates were incubated for 1 hour on ice to prevent sialic acid recycling from interfering with the assay. Media containing unbound virus was then discarded, and replaced with 200 μ L of complete media and plates were incubated at 37°C with 5% CO₂ for an additional 45 h. Cells were then washed with 200 μ L PBS. 5X reporter lysis buffer (Promega, Southampton, UK) was diluted in sterile ddH₂O and 100 μ L was added per well. Plates were then frozen at -80°C. Samples were thawed and 10 μ L of lysate per well was used for a Bicinchoninic Acid Assay (BCA assay). A standard curve of Bovine Serum Albumin (BSA) standards at concentrations 0.025, 0.125, 0.25, 0.5, 0.75, 1.0, 1.5, and 2.0 mg/mL was created. Lysate and standards were incubated for 1 hour at 37°C with 5% CO₂ after the addition of 100 μ L working reagent (ThermoFisher Scientific, Waltham, USA). Absorbance was measured at 570 nm on a plate reader (BioRad, Watford, UK).

To assay for luciferase activity, 100 μ L luciferase assay substrate (Promega, Southampton, UK) was added to 20 μ L of the thawed cell lysate in white 96 well plates. Luminescence was quantified using a Clariostar Plus plate reader (BMG, Birmingham, UK). Luminescence was normalised against protein concentration, to give a final value in relative light units (RLU) per milligram (mg) or microgram (μ g) of protein.

Evaluation of CAR binding by HAdV-D fiber knob proteins

CHO cells stably expressing CAR (CHO-CAR) cells were seeded at 2×10^4 cells per well in 96 well V-bottomed plates. Diluted recombinant fiber knob proteins corresponding to species D adenoviruses at varying concentrations were applied to the appropriate wells. The cells and fiber knob proteins were incubated for 1 h at 4°C. Wells were made up to 200 μ L volume and cells were pelleted at 1400 RPM for 4 min. The supernatant was removed and 200 μ L PBS was added to each well. Cells were pelleted again at 1400 RPM for 4 minutes and the supernatant discarded. 50 μ L of primary antibody (05-644 Anti-CAR clone RmcB, Lot 3022897, EMD Millipore, MA, USA) was added to each well and the cells were incubated on ice at 4°C for 1 h.

The volume was again made up to 200 μ L before cells were pelleted at 1400 RPM for 4 minutes. The supernatant was removed, and 200 μ L PBS added before cells were pelleted using the same process and the supernatant again discarded. 50 μ L secondary antibody (Goat Anti-Mouse IgG H&L (Alexa Fluor-488), product code: ab150113) was added and the cells were incubated on ice for 30 min at 4°C. Cells were again pelleted for 4 min by centrifugation at 1400RPM, before being washed with 200 μ L PBS and pelleted using the same conditions. 100 μ L PFA was added to each well and the plate was left for 10–15 min. 100 μ L PBS was added on top of the PFA before another centrifugation step. The supernatant was removed and a further wash and centrifugation step performed. Cells were finally resuspended in 200 μ L PBS and data was collected on an Attune flow cytometer (Invitrogen,

ThermoFisher Scientific, Waltham, USA). IC₅₀ values were calculated using GraphPad Prism⁴⁶.

Statistics

RLU data from the neuraminidase assay was analysed by an unpaired, non-parametric, two-sided Mann-Whitney test in GraphPad Prism Version 9.5.1⁴⁶. There were four replicates per condition ($n = 4$) with an assumption of non-normally distributed data. Any results with a p -value of less than 0.05 were deemed a statistically significant reduction in infection in the presence of the neuraminidase.

DATA AVAILABILITY

Crystallographic data from this manuscript is available via the protein data bank for structures with PDB IDs: 8OFQ, 8OFR, 8OFP, 6STW, 6STV, 6STT, 6STU, 8OFS, 8OFT, 8OFU and 8OFV. All other data is available upon reasonable request from the authors.

Received: 7 June 2023; Accepted: 27 July 2023;

Published online: 26 September 2023

REFERENCES

- Buckwalter, S. P. et al. Real-time qualitative PCR for 57 human adenovirus types from multiple specimen sources. *J. Clin. Microbiol.* **50**, 766–771 (2012).
- Human Adenovirus Working Group. *Home - July 2019 Update*, <<http://hadvvg.gmu.edu/index.php/criteria-for-a-new-hadv-type/>> (2019).
- Stepanenko, A. A. & Chekhonin, V. P. Tropism and transduction of oncolytic adenovirus 5 vectors in cancer therapy: Focus on fiber chimerism and mosaicism, hexon and pIX. *Virus Res.* **257**, 40–51 (2018).
- Pérez-Illana, M. et al. Cryo-EM structure of enteric adenovirus HAdV-F41 highlights structural variations among human adenoviruses. *Sci. Adv.* **7**, eabd9421 (2021).
- Abbink, P. et al. Comparative seroprevalence and immunogenicity of six rare serotype recombinant adenovirus vaccine vectors from subgroups B and D. *J. Virol.* **81**, 4654–4663 (2007).
- Parker, A. L. et al. Effect of neutralizing sera on Factor X-mediated adenovirus Serotype 5 gene transfer. *J. Virol.* **83**, 479–483 (2009).
- Waddington, S. N. et al. Adenovirus serotype 5 hexon mediates liver gene transfer. *Cell* **132**, 397–409 (2008).
- Parker, A. L. et al. Multiple vitamin K-dependent coagulation zymogens promote adenovirus-mediated gene delivery to hepatocytes. *Blood* **108**, 2554–2561 (2006).
- Shayakhmetov, D. M., Gaggari, A., Ni, S., Li, Z.-Y. & Lieber, A. Adenovirus binding to blood factors results in liver cell infection and hepatotoxicity. *J. Virol.* **79**, 7478–7491 (2005).
- Toovey, O. T. R. et al. An outbreak of adenovirus D8 keratoconjunctivitis in Leicester, United Kingdom, from March to August 2019. *J. Med. Virol.* <https://doi.org/10.1002/jmv.26647> (2020).
- Ghebremedhin, B. Human adenovirus: Viral pathogen with increasing importance. *Eur. J. Microbiol. Immunol.* **4**, 26–33 (2014).
- Baker, A. T., Mundy, R. M., Davies, J., Rizkallah, P. J. & Parker, A. L. Adenovirus serotype 26 utilises sialic acid bearing glycans as a primary cell entry receptor. *Sci. Adv.* **5** <https://doi.org/10.1126/sciadv.aax3567> (2019).
- Baker, A. T. et al. Diversity within the adenovirus fiber knob hypervariable loops influences primary receptor interactions. *Nat. Commun.* **10**, 741 (2019).
- Milligan, I. D. et al. Safety and Immunogenicity of Novel Adenovirus Type 26- and Modified Vaccinia Ankara-Vectored Ebola Vaccines: A Randomized Clinical Trial. *JAMA: J. Am. Med. Asso.* **315**, 1610–1623 (2016).
- Stephenson, K. E. et al. First-in-human randomized controlled trial of an oral, replicating adenovirus 26 vector vaccine for HIV-1. *PLoS One* **13**, e0205139 (2018).
- Stephenson, K. E. et al. Immunogenicity of the Ad26.COVS.2 Vaccine for COVID-19. *J. Am. Med. Asso.* **325**, 1535–1544 (2021).
- Arnberg, N., Edlund, K., Kidd, A. H. & Wadell, G. Adenovirus type 37 uses sialic acid as a cellular receptor. *J. Virol.* **74**, 42–48 (2000).
- Burmeister, W. P., Guilligay, D., Cusack, S., Wadell, G. & Arnberg, N. Crystal structure of species D adenovirus fiber knobs and their sialic acid binding sites. *J. Virol.* **78**, 7727–7736 (2004).
- Chandra, N. et al. Sialic acid-containing glycans as cellular receptors for ocular human adenoviruses: implications for tropism and treatment. *Viruses* **11**, 395 (2019).
- Varki, A. Sialic acids in human health and disease. *Trends Mol. Med.* **14**, 251–360 (2008).

21. Bergelson, J. M. et al. Isolation of a Common Receptor for Coxsackie B Viruses and Adenoviruses 2 and 5. *Science (American Association for the Advancement of Science)* **275**, 1320–1323 (1997).
22. Bates, E. A. et al. Development of a low-seroprevalence, $\alpha v\beta 6$ integrin-selective virotherapy based on human adenovirus type 10. *Mol. Ther. Oncolytics* **25**, 43–56 (2022).
23. Matrosovich, M., Herrler, G. & Dieter Klenk, H. Sialic Acid Receptors of Viruses. *SialioGlyco Chem. Biol.* **11**, 1–28 (2015).
24. Lenman, A. et al. Human Adenovirus 52 Uses Sialic Acid-containing Glycoproteins and the Coxsackie and Adenovirus Receptor for Binding to Target Cells. *PLoS Pathogens* **11**, e1004657 (2015).
25. Kumlin, U., Olofsson, S., Dimock, K. & Arnberg, N. Sialic acid tissue distribution and influenza virus tropism. *Influenza Other Resp. Viruses* **2**, 147–154 (2008).
26. Jonas, R. A., Ung, L., Rajaiya, J. & Chodosh, J. Mystery eye: Human adenovirus and the enigma of epidemic keratoconjunctivitis. *Prog. Retinal Eye Res.* **76**, 100826–100826 (2020).
27. Pettit, T. H. & Holland, G. N. Chronic Keratoconjunctivitis Associated with Ocular Adenovirus Infection. *Am. J. Ophthalmol.* **88**, 748–751 (1979).
28. Walsh, M. P. et al. Evidence of molecular evolution driven by recombination events influencing tropism in a novel human adenovirus that causes epidemic keratoconjunctivitis. *PLoS one* **4**, e5635–e5635 (2009).
29. Aoki, K. et al. Epidemic Keratoconjunctivitis Due to the Novel Hexon-Chimeric-Intermediate 22,37/H8 Human Adenovirus. *J. Clin. Microbiol.* **46**, 3259–3269 (2008).
30. Zhou, X. et al. Analysis of human adenovirus type 19 associated with epidemic keratoconjunctivitis and its reclassification as adenovirus type 64. *Investigative ophthalmology & visual science* **53**, 2804–2811 (2012).
31. U.S. Food and Drug Administration. *FDA D.I.S.C.O. Burst Edition: FDA approval of Adstiladlin (nadofaragene firadenovec-vncg) for patients with high-risk Bacillus Calmette-Guérin unresponsive non-muscle invasive bladder cancer with carcinoma in situ with or without papillary tumors*, <<https://www.fda.gov/drugs/resources-information-approved-drugs/fda-disco-burst-edition-fda-approval-adstiladlin-nadofaragene-firadenovec-vncg-patients-high-risk>> (2022).
32. Wu, S. et al. Safety, tolerability, and immunogenicity of an aerosolised adenovirus type-5 vector-based COVID-19 vaccine (Ad5-nCoV) in adults: preliminary report of an open-label and randomised phase 1 clinical trial. *The Lancet Infectious Dis.* **21**, 1654–1664 (2021).
33. Marttila, M. et al. CD46 Is a Cellular Receptor for All Species B Adenoviruses except Types 3 and 7. *J. Virol.* **79**, 14429–14436 (2005).
34. Wang, H. et al. Desmoglein 2 is a receptor for adenovirus serotypes 3, 7, 11 and 14. *Nat. Med.* **17**, 96–104 (2011).
35. Nilsson, E. C. et al. The GD1a glycan is a cellular receptor for adenoviruses causing epidemic keratoconjunctivitis. *Nat. Med.* **17**, 105–109 (2011).
36. Uusi-Kerttula, H. et al. Pseudotyped $\alpha v\beta 6$ integrin-targeted adenovirus vectors for ovarian cancer therapies. *Oncotarget* **7**, 27926–27937 (2016).
37. Mendonça, S. A., Lorincz, R., Boucher, P. & Curiel, D. T. Adenoviral vector vaccine platforms in the SARS-CoV-2 pandemic. *npj vaccines* **6**, 97–97 (2021).
38. Baden, L. R. et al. Safety and immunogenicity of two heterologous HIV vaccine regimens in healthy, HIV-uninfected adults (TRAVVERSE): a randomised, parallel-group, placebo-controlled, double-blind, phase 1/2a study. *The Lancet HIV* **7**, e688–e698 (2020).
39. Pollard, A. J. et al. Safety and immunogenicity of a two-dose heterologous Ad26.ZEBOV and MVA-BN-Filo Ebola vaccine regimen in adults in Europe (EBO-VAC2): a randomised, observer-blind, participant-blind, placebo-controlled, phase 2 trial. *The Lancet Infectious Dis.* **21**, 493–506 (2021).
40. Persson, B. D. et al. Human species D adenovirus hexon capsid protein mediates cell entry through a direct interaction with CD46. *Proc. Natl. Acad. Sci. USA* **118**, e2020732118 (2021).
41. Kabsch, W. XDS. *Acta Crystallographica Sec. D Biol. Crystallogr.* **66**, 125–132 (2010).
42. Winter, G. DIALS: implementation and evaluation of a new integration package. *Acta Crystallographica Sec. D* **74**, 85–97 (2018).
43. Dodson, E. J., Winn, M. & Ralph, A. Collaborative computational project, number 4: Providing programs for protein crystallography. *Methods Enzymol.* **277**, 620–633 (1997).
44. The PyMOL Molecular Graphics System, Version 2.0.
45. Madeira, F. et al. Search and sequence analysis tools services from EMBL-EBI in 2022. *Nucleic Acids Res.* **50**, W276–W279 (2022).
46. GraphPad Prism version 9.4.1 for Windows (San Diego, California USA).

ACKNOWLEDGEMENTS

The authors would like to thank Diamond Light Source for beamtime (proposals mx18812, mx20147 and mx29990), and the staff of beamlines I03, I04 and I04-1 for assistance with crystal testing and data collection. R.M.M. was supported in part by grant MR/N0137941/1 for the GW4 BIOMED MRC DTP, awarded to the Universities of Bath, Bristol, Cardiff and Exeter from the Medical Research Council (MRC)/UKRI. A.T.B. was supported by a Tenovus Cancer Care Ph.D. studentship to A.L.P. (ref PhD2015/L13). E.A.B. is funded by a Cardiff University Ph.D. studentship to A.L.P. and by the Experimental Cancer Medicine Centre award to Cardiff University (reference C7838/A25173). T.G.C. was funded by Knowledge Economy Skills Scholarships (KESS 2) Ph.D. studentship award (Reference 515374). A.T-C is funded by A PhD studentship from Cancer Research Wales (reference 514472). E.M. was supported by a Wellcome Trust ISSF Translational Kickstarter Award to A.L.P. (reference 517732) and by Velindre Charitable Funds (reference 519006). P.J.R. and A.L.P. are funded by HEFCW.

AUTHOR CONTRIBUTIONS

R.M.M. and A.T.B. and P.J.R. performed the protein production and crystallisation. Analysis of structural outputs was performed by R.M.M., A.T.B., and P.J.R.; R.M.M. and E.A.B. performed biological studies with input from T.G.C., A.T.-C., and E.M.; R.M.M., P.J.R., and A.L.P. analysed the data. A.L.P. supervised the study and was responsible for funding acquisition. R.M.M., P.J.R., and A.L.P. wrote the original manuscript draft, and all authors read and reviewed this manuscript.

COMPETING INTERESTS

A.L.P. is founder and CSO of Trocept Therapeutics. All other authors declare that they have no competing interests.

ADDITIONAL INFORMATION

Supplementary information The online version contains supplementary material available at <https://doi.org/10.1038/s44298-023-00001-5>.

Correspondence and requests for materials should be addressed to Pierre J. Rizkallah or Alan L. Parker.

Reprints and permission information is available at <http://www.nature.com/reprints>

Publisher's note Springer Nature remains neutral with regard to jurisdictional claims in published maps and institutional affiliations.



Open Access This article is licensed under a Creative Commons Attribution 4.0 International License, which permits use, sharing, adaptation, distribution and reproduction in any medium or format, as long as you give appropriate credit to the original author(s) and the source, provide a link to the Creative Commons license, and indicate if changes were made. The images or other third party material in this article are included in the article's Creative Commons license, unless indicated otherwise in a credit line to the material. If material is not included in the article's Creative Commons license and your intended use is not permitted by statutory regulation or exceeds the permitted use, you will need to obtain permission directly from the copyright holder. To view a copy of this license, visit <http://creativecommons.org/licenses/by/4.0/>.

© The Author(s) 2023